

MAN: Multi-Action Networks Learning

Keqin Wang¹ Alison Bartsch¹ Amir Barati Farimani¹

Abstract— Learning control policies with large action spaces is a challenging problem in the field of reinforcement learning due to present inefficiencies in exploration. In this work, we introduce a Deep Reinforcement Learning (DRL) algorithm called Multi-Action Networks (MAN) Learning that addresses the challenge of large discrete action spaces. We propose separating the action space into two components, creating a Value Neural Network for each sub-action. Then, MAN uses temporal-difference learning to train the networks synchronously, which is simpler than training a single network with a large action output directly. To evaluate the proposed method, we test MAN on a block stacking task, and then extend MAN to handle 12 games from the Atari Arcade Learning environment with 18 action spaces. Our results indicate that MAN learns faster than both Deep Q-Learning and Double Deep Q-Learning, implying our method is a better performing synchronous temporal difference algorithm than those currently available for large action spaces.

I. INTRODUCTION

Learning a policy with a large discrete action space is a current challenge for control tasks. Specifically in reinforcement learning (RL), large action spaces impede performance. In particular, DQN [1] [2], and other similar algorithms have difficulty handling large action spaces. Unfortunately, large action spaces are very prevalent, e.g. a control task in continuous action space can be solved by discretizing the actions creating a large discrete action space. Moreover, some learning pipelines may use images, where each image pixel is an action. These problems are challenging due to the large exploration space, i.e. there are numerous actions to choose from.

Currently, one of the common methods developed to address the challenge of large action spaces is to reduce the dimension of the action space by introducing features and approximating actions [3]. These methods require additional models to map between features and actions, which is both time consuming and introduces new error into the mappings. Another famous approach is to learn the policy directly, e.g. policy-gradient methods [4]. However, the computations in policy-gradient methods are more complicated than value-iteration methods.

In this paper, we present a novel DRL algorithm known as *Multi-Action Networks* (MAN) Learning, leveraging DQN and the powerful capabilities of temporal difference (TD) learning [5]. Our method addresses the challenge of large discrete action spaces by splitting the original large action space into two smaller sub-action spaces. Instead of depending on a single value network with a large output layer, we

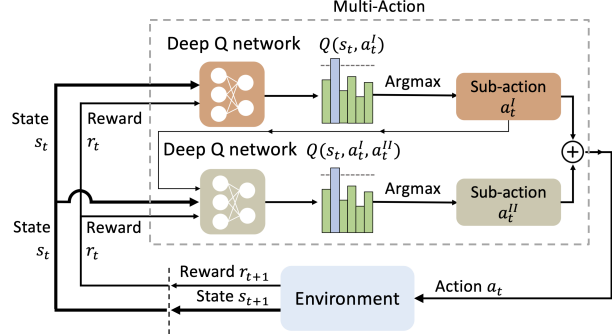


Fig. 1. MAN structure schematic. The MAN firstly splits the original action a_t into two sub-actions a_t^I and a_t^{II} ; and then uses two streams to separately estimate values of sub-actions; finally combines these sub-actions back to the original action. Both networks output Q-values for each action. Viewing the content in the dashed box as a whole is the traditional reinforcement learning pipeline.

break this into two value networks each with smaller output layers. Figure 1 delineates the separate process. The original action becomes a combination of the two sub-actions. For example, finding the position of a target object in a 2-D image can be decomposed into determining the position along the horizontal axis first, and then along the vertical axis. In many cases, what was originally the product of two actions is now reduced to the sum of two actions, decreasing the potential action space dramatically. This approach allows us to search for the optimal policy within two much smaller action spaces, which saves exploration time. We evaluate MAN on both block stacking and Atari tasks, comparing our model’s performance to both DQN and DDQN [6]. We find that our proposed method outperforms both DQN and DDQN in terms of both the learning speed and the final score. The implementation of MAN is available at <https://github.com/keqinw/MAN>.

II. RELATED WORK

Value function approximation is one of the common approaches in RL. One of the earliest successful pioneers was TD(λ), an online value function approximation algorithm that reached expert-level performance in Backgammon in the early 1990s [7]. Q-learning [8] [9] is directly derived from TD(0), where for each update step, Q-learning adopts the greedy policy $\max_a Q(S_{t+1}, a)$.

Deep Q-Network (DQN) learning [1] [2] was the first work that successfully incorporated deep neural networks with reinforcement learning, creating an algorithm which was able to learn successful control policies for a wide range of classic Atari 2600 video games. In this work, researchers

¹Department of Mechanical Engineering, Carnegie Mellon University, United States

also addressed the fundamental instability challenge associated with using neural networks with RL by leveraging two techniques: experience replay and target networks. The development of DQN ignited the field of DRL, and led to numerous future works that presented modifications of the original DQN algorithm.

Many algorithms optimize DQN from the Q-function perspective. A simple improvement to the original algorithm is Double DQN (DDQN) [6], which introduces a frozen network to mitigate the over-optimism the single network of DQN accumulates. In this work, we use DDQN for this reason. Dueling DQN [10] is a modification that learns the value $V(s)$ and advantage $A(s, a)$ functions with a single model. Other popular algorithms that use update function optimization are: Rainbow [11], Fast reward propagation [12], Deep Recurrent Q-Network (DRQN) [13], averaged-DQN [14] and DQV [15].

Some modifications to DQN focus instead on the reward function. To address the challenge of generalization and robustness with DQN, Soft DQN [16] is an entropy-regularized modification that introduces KL-divergence and entropy into the reward function. DQN with Pop-art [17] created an adaptive normalized reward which helped the model adapt to different Atari games.

Another fundamental problem within DRL is the exploration/exploitation trade-off. The most basic strategy to balance exploration and exploitation is ϵ -greedy. However, there are more reliable methods for efficient exploration such as Distributional DRL. C51 [18] focuses on the distribution of value and designs a distributional DQN algorithm. Bootstrapped DQN [19] uses Bayesian neural networks, explores via the posterior sampling of Q-functions. Implicit Quantile Networks (IQN) [20] add uncertainty by using quantile regression to learn the distribution over returns of the current policy. Other popular algorithms which concentrate on distributional RL are: QR-DQN [21], Ape-X DQN [22] and Ape-X DQfD [23]. An alternate method of overcoming exploration challenges is to leverage human examples. Deep Q-learning from Demonstrations (DQfD) [24] utilizes small sets of demonstrations to dramatically accelerate learning.

Another avenue to improve the performance of these algorithms is to focus on computational resources themselves. General Reinforcement Learning Architecture (Gorila) [25] is the first massively distributed architecture for DRL. The key intuition is that Gorila leverages massive computational resources as opposed to a single CPU/GPU. Other popular algorithms that aim to maximize and optimize computational resources are: Clemente *et al.* [26], Stooke *et al.* [27].

In this work, we present a novel improvement to DQN: reducing the difficulty of exploration by splitting the original action with a large action space into two smaller sub-actions. This method is both simple and innovative and works well in especially large action spaces where alternative DQN-based methods are prone to failure.

III. PRELIMINARIES

We consider a Markov Decision Process (MDP), defined by the tuple $(\mathcal{S}, \mathcal{A}, \mathcal{P}, r, T, \gamma)$, where \mathcal{S} denotes a set of possible states, \mathcal{A} denotes a set of potential actions, \mathcal{P} denotes the transition dynamics $\mathcal{P} : \mathcal{S} \times \mathcal{A} \times \mathcal{S} \rightarrow [0, 1]$, $r(s, a)$ as the reward function, T as the task horizon, γ as a discount factor $\gamma \in [0, 1]$. The goal of reinforcement learning is to search the optimal policy π^* which maximizes the expected discounted reward:

$$\pi^* = \arg \max_{\pi} \mathbb{E}_{\rho_{\pi}} \left[\sum_{t=0}^T \gamma^t r(s_t, a_t) \right]$$

where ρ_{π} is the state-action distribution.

A. Deep Q-networks (DQN)

Our approach takes its inspiration from DQN [2], which uses a deep Q-network to approximate the high dimensional value functions. Here is the objective function at iteration i :

$$L_i(\theta_i) = \mathbb{E}_{s, a, r, s'} \left[\left(y_i^{DQN} - Q(s, a; \theta_i) \right)^2 \right]$$

with

$$y_i^{DQN} = r + \gamma \max_{a'} Q(s', a'; \theta_i^-)$$

where $Q(s', a'; \theta)$ is the Q-network parameterized with θ , and θ^- represents the parameters of a fixed and separate **target network**.

This method performs poorly in practice, especially with more complex tasks, such as the Atari 2600 games. To overcome this issue with DQN, researchers created target networks to stabilize the learning by temporally freezing the parameters of the target network $Q(s', a'; \theta_i^-)$, and periodically updating it with the parameters of the main network $Q(s', a'; \theta)$. The specific gradient update is

$$\nabla_{\theta_i} L_i(\theta_i) = \mathbb{E}_{s, a, r, s'} \left[\left(y_i^{DQN} - Q(s, a; \theta_i) \right) \nabla_{\theta_i} Q(s, a; \theta_i) \right].$$

Another key ingredient behind the success of DQN is **experience replay** [28]. As the agent explores the environment, it populates a replay buffer $D_t = (e_1, e_2, \dots, e_t)$ with its experiences, where transition $e_t = (s_t, a_t, r_t, s'_t)$. To optimize the networks, transitions are randomly sampled from the replay buffer. The sequence of losses thus takes the form

$$L_i(\theta_i) = \mathbb{E}_{s, a, r, s' \sim D} \left[\left(y_i^{DQN} - Q(s, a; \theta_i) \right)^2 \right].$$

This random sampling decorrelates the training data, resulting in more robust training. Additionally, it increases data efficiency by re-using the experience samples.

B. Double Deep Q-networks (DDQN)

The previous section described the main components of DQN as presented in the work of Mnih *et al.*, 2015. In this work, we use the improved Double DQN (DDQN) learning algorithm of van Hasselt *et al.*, 2016. In Q-learning and DQN, the max operator uses the same values to both select and evaluate an action, which will therefore lead to overly

optimistic value estimates [29]. To alleviate this problem, DDQN uses the following evaluation:

$$y_i^{DDQN} = r + \gamma Q(s', \arg \max_{a'} Q(s', a'; \theta_i); \theta_i^-)$$

IV. MAN: MULTI-ACTION NETWORKS LEARNING

We now introduce our novel DRL algorithm called Multi-Action Networks (MAN) learning. We first present the online RL algorithm based on $TD(\lambda)$ together with its update rules, and then extend these update rules to objective functions that can be used to train Artificial Neural Networks (ANNs) for solving complex RL problems.

A. Multi-Action learning based on Q -learning

The main idea of Multi-Action (MA) learning is to split the original action into two sub-actions, thus replacing a larger action space with two smaller action spaces. For example, in Go, where the original action is 361 coordinate points on the board, we can divide it into two sub-actions, first the horizontal position coordinates(19 actions) and then the vertical position coordinates(19 actions).

The Multi-Action Learning framework is suitable to large action space problems, which separates the action space into two smaller parts. The formal definition is shown below.

Definition 1. *Multi-Action learning is characterized by:*

- (1) *initial action space: $\mathcal{A} = (\mathcal{A}^I, \mathcal{A}^{II})$,*
- (2) *two sub-actions: $a^I \in \mathcal{A}^I, a^{II} \in \mathcal{A}^{II}$,*
- (3) *reward function: $r = r(s, a^I, a^{II})$,*
- (4) *action values of sub-actions: $Q^I(s, a^I), Q^{II}(s, a^I, a^{II})$,*
- (5) *transition: (s, a^I, a^{II}, r, s') .*

It is important to note that we execute the sub-actions sequentially to complete the overall action \mathcal{A} . This means there is a dependency between the sub-actions, i.e., the latter sub-action a^{II} is selected based on the completion of the previous sub-action a^I . In other words, the information of a^I will be used as input for the a^{II} along with the state s .

We combine this main idea of sub-actions with the $TD(\lambda)$ method presented in [5] to update the values of sub-actions. According to the $TD(\lambda)$ method, after interacting with the environment and collecting a transition $(s_t, a_t^I, a_t^{II}, r_t, s_{t+1})$, multi-action updates the Q^{II} function as:

$$Q^{II}(s_t, a_t^I, a_t^{II}) := (1 - \alpha)Q^{II}(s_t, a_t^I, a_t^{II}) + \alpha[r_t + \gamma \max_{a_{t+1}^I, a_{t+1}^{II} \in \mathcal{A}} Q^{II}(s_{t+1}, a_{t+1}^I, a_{t+1}^{II})] \quad (1)$$

However, it is challenging to get the maximum value with respect to a^I and a^{II} at the same time. Another problem arises when updating Q^I as the action is not fully executed until the agent has executed both a^I and a^{II} . Therefore, in order to link a^I with its ‘future’ reward, we need to add an artificial condition, see as Definition 2.

Definition 2. *The value of the previous action equals the maximum value of the next action predicated on this previous action, such that*

$$Q^I(s, a^I) = \max_{a^{II} \in \mathcal{A}^{II}} Q^{II}(s, a^I, a^{II})$$

Based on Definition 2, we can derive two lemmas.

Lemma 1. *The Q value of a^I is the V value of a^{II} , such that*

$$\begin{aligned} Q^I(s, a^I) &= \max_{a^{II} \in \mathcal{A}^{II}} Q^I(s, a^I, a^{II}) \\ &= V^{II}(s, a^I) \end{aligned}$$

where $V^{II}(s, a^I)$ is the state value.

Lemma 2.

$$\max_{a^I \in \mathcal{A}^I} Q^I(s, a^I) = \max_{a^I, a^{II} \in \mathcal{A}} Q^I(s, a^I, a^{II})$$

The V value update rule in $TD(\lambda)$ is:

$$V(s_t) := (1 - \alpha)V(s_t) + \alpha[r_t + \gamma V(s_{t+1})] \quad (2)$$

With Lemma 1, we can rewrite the Equation 2 by replacing $V(s_t)$ with $Q(s_t, a_t)$:

$$Q^I(s_t, a_t^I) := (1 - \alpha)Q^I(s_t, a_t^I) + \alpha[r_t + \gamma Q^I(s_{t+1}, a_t^I)] \quad (3)$$

We have ‘tentatively’ obtained the Equation 3 as the value update function for Q^I . However, in practice, we find that the model converges very slowly. An alternative module replaces the $Q^I(s_{t+1}, a_t^I)$ in Equation 3 as:

$$Q^I(s_t, a_t^I) := (1 - \alpha)Q^I(s_t, a_t^I) + \alpha[r_t + \gamma \max_{a^{II} \in \mathcal{A}^{II}} Q^{II}(s_{t+1}, a_t^I, a_{t+1}^{II})] \quad (4)$$

The Equation 4 is as the same as the Equation 3 mathematically according to the Definition 2, nevertheless the practical result shows that Equation 4 is better. This is perhaps due to the fact that the Q^I action is not executed until the end, meaning it has not yet interacted with the environment, while Q^{II} is the result of a real interaction with the environment. Thus, Q^{II} is always corrected with a “ground true” value, but there is a bias in Q^I . According to the above view, we eventually chose Equation 4 to update Q^I .

With Lemma 2, we rewrote the update function of Q^{II} (Equation 1) as:

$$Q^{II}(s_t, a_t^I, a_t^{II}) := (1 - \alpha)Q^{II}(s_t, a_t^I, a_t^{II}) + \alpha[r_t + \gamma \max_{a_{t+1}^I \in \mathcal{A}^I} Q^I(s_{t+1}, a_{t+1}^I)] \quad (5)$$

In Equation 5, instead of finding the maximum value over both a_{t+1}^I and a_{t+1}^{II} , we turn to the maximum value over a_{t+1}^I only.

B. Multi-Action Networks learning

Here we show how to transform the update rules 4 and 5 as objective functions to train ANNs, and how to make the training procedure stable with the use of ‘Experience Replay’ and ‘Double Networks’.

We define a neural network Q^I with parameter θ and a neural network Q^{II} with parameter ζ to approximate the value functions of a^I and a^{II} respectively. In order to build the two objective functions it is possible to simply express MAN-Learning’s update rules in Mean Squared Error terms similarly to how DQN addresses the Q-Learning updating.

The **objective function** of θ is:

$$\begin{aligned} Loss_{\theta} = & \\ \mathbb{E}[(r_t + \gamma \max_{a_{t+1}^{II} \in \mathcal{A}^{II}} Q^{II}(s_{t+1}, a_t^I, a_{t+1}^{II}) - Q^I(s_t, a_t^I))^2] \end{aligned} \quad (6)$$

The **objective function** of ζ is:

$$\begin{aligned} Loss_{\zeta} = & \\ \mathbb{E}[(r_t + \gamma \max_{a_{t+1}^I \in \mathcal{A}^I} Q^I(s_{t+1}, a_{t+1}^I) - Q^{II}(s_t, a_t^I, a_{t+1}^{II}))^2] \end{aligned} \quad (7)$$

Experience buffer: it consists of a memory buffer D , of size M , in which experiences are stored in the form $(s_t, a_t^I, a_t^{II}, r_t, s_{t+1})$. Notice there is a slight difference with traditional MDP experience that we store the sub-actions here.

Double Networks: here we inherit the method in DDQN to reduce the overestimations which can impede learning an optimal policy.

We have now defined all elements of our novel DRL algorithm which is summarized by the pseudocode presented in Algorithm 1.

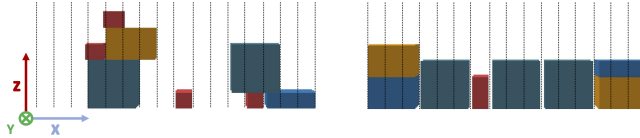


Fig. 2. Stacking mission statement: there are four sizes of blocks to choose from. The dotted line divides 16 areas, of which the middle 14 can be used to place blocks. Left: A case of random stacking. Right: A case of tight stacking. Tight means the blocks are compact and the overall height of them are low.

V. EXPERIMENTS

We now show the practical performance of the MAN learning by starting with a simple stacking task and then showing larger scale results for general Atari game-playing.

A. Block Stacking

We first evaluate the performance of the MAN architecture on a simple stacking task. This particular task is useful to illustrate the key ideas of our algorithm, since it is natural to divide the original action space into selecting the block type and selecting the block position. The goal of this task is to stack rectangular blocks of four different sizes together while making them both as compact as possible and with the lowest overall height possible. Specifically, as shown in Figure 2, the block positions vary in the x and z dimensions. We assume blocks have the same width in the y-axis, allowing them to be stacked easily. No rotation is allowed for this simple task. As for observation state, we uniformly discretize the stacking area into 16 positions along x-axis with width 1. The state S_t is defined as the heights of the block outlines in these 16 discrete spaces. As for the stacking action, we need to choose both which type of blocks to stack and where

Algorithm 1 MAN Learning

```

1: Input: Set update frequency  $K$ , minibatch  $N$ , learning
   rate  $\alpha$ , epsilon  $e$ , episode,  $t = 0$ ,  $\Delta^I = 0$ ,  $\Delta^{II} = 0$ ;
2: Input:  $Q^I$  network with parameters  $\theta$  and  $\theta^-$ 
3: Input:  $Q^{II}$  network with parameters  $\zeta$  and  $\zeta^-$ 
4: for  $t = 1$  to  $episode$  do
5:   Observe  $S_t$ 
6:   Choose  $A_t^I \sim \pi_{\theta}^I(S_t)$ 
7:   Choose  $A_t^{II} \sim \pi_{\zeta}^{II}(S_t, A_t^I)$ 
8:   Get  $R_t, S_{t+1}$ 
9:   Store  $(S_t, A_t^I, A_t^{II}, R_t, S_{t+1})$  in buffer  $D$ 
10:  for  $j = 1$  to  $N$  do
11:    Sample transition  $j$  from buffer  $D$ 
12:    if  $S_{j+1}$  is over then
13:       $y_j^I = r_j$ 
14:       $y_j^{II} = r_j$ 
15:    else
16:       $A_{next}^I = \arg \max_{a^I} (Q^I(S_{j+1}; \theta))$ 
17:       $A_{next}^{II} = \arg \max_{a^{II}} (Q^{II}(S_{j+1}, A_j^I; \zeta))$ 
18:       $y_j^I = r_j + \gamma Q^{II}(S_{j+1}, A_j^I, A_{next}^{II}; \zeta^-)$ 
19:       $y_j^{II} = r_j + \gamma Q^I(S_{j+1}, A_{next}^I; \theta^-)$ 
20:    end if
21:     $\delta_j^{\theta} = (y_j^I - Q^I(S_{j+1}, A_j^I; \theta))^2$ 
22:     $\delta_j^{\zeta} = (y_j^{II} - Q^{II}(S_{j+1}, A_j^I, A_j^{II}; \zeta))^2$ 
23:    Accumulate change:
24:     $\Delta^I \leftarrow \Delta^I + \delta_j^{\theta} \cdot \nabla_{\theta} Q^I(S_{j+1}, A_j^I; \theta)$ 
25:     $\Delta^{II} \leftarrow \Delta^{II} + \delta_j^{\zeta} \cdot \nabla_{\zeta} Q^{II}(S_{j+1}, A_j^I, A_j^{II}; \zeta)$ 
26:  end for
27:  Update weights:
28:   $\theta \leftarrow \theta + \alpha \cdot \Delta^I$ , reset  $\Delta^I = 0$ 
29:   $\zeta \leftarrow \zeta + \alpha \cdot \Delta^{II}$ , reset  $\Delta^{II} = 0$ 
30:  if  $t \equiv 0 \bmod K$  then
31:     $\theta^- := \theta$ 
32:     $\zeta^- := \zeta$ 
33:  end if
34: end for

```

to place the block. Here we design four types of blocks with the sizes of $1 \times 1 \times 1$, $1 \times 3 \times 1$, $2 \times 3 \times 1$ and $3 \times 3 \times 1$ respectively. The position selection action sub-space is defined as the middle 14 positions of the stacking area. The leftmost and rightmost positions are not included in this action space since most of blocks in our tasks are of 3 width (if placed in the edge, a part of block will out of environmental bounds). The product of the number of block types (4) and the number of placing positions (14) yields 56 total actions.

Existing algorithms, such as DQN and Double-DQN will have difficulty handling 56 potential actions, because this large action space requires a significant amount of exploration time. However, with MAN this action space is decoupled into block type selection and then block placement, reducing the 56 actions to 18 (4+14) actions, requiring less exploration time and simplifying the task.

In practice, we use two structurally similar networks (Q^I ,

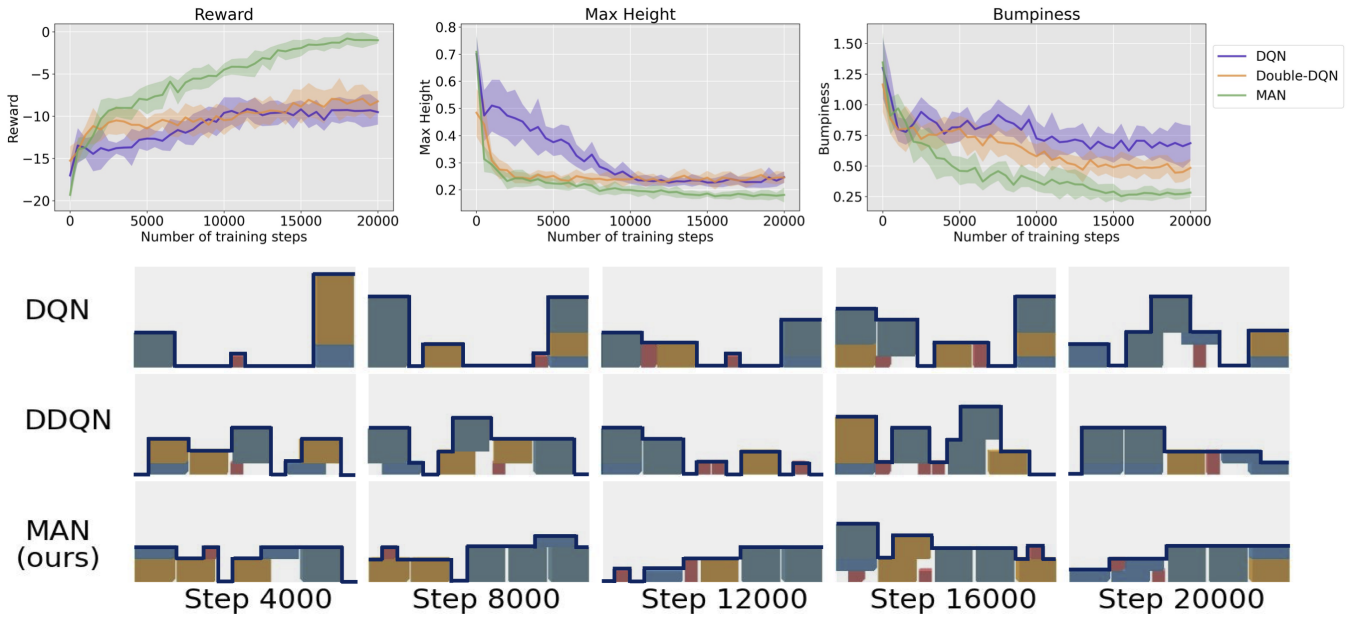


Fig. 3. Top: Performances of MAN compared with DQN and DDQN. Bottom: Images of piles captured in testing experiments. The outline of pile is marked in dark blue line.

Q^{II}) to predict the blocks type (a^I) and the placement of blocks (a^{II}) separately. Specifically, Q^I and Q^{II} share the two identical hidden layer (256x512, 512x256) and activation function (Rectified Linear Unit (ReLU)), with the following differences: first, the number of neurons in their output layer is 4 and 14, corresponding to their respective action subspace dimensions; second, Q^{II} receives additional information due to the sequence between a^I and a^{II} , specifically the input layer of Q^{II} has 3 more neurons than Q^I (3 neurons here represent the outline of selected blocks, e.g., the outline of 3x1x1 blocks is (1,1,1), and the outline of 1x1x1 blocks is (0,1,0)).

To compare the performance, we also implemented DQN and DDQN, the network structures of which are similar to that of Q^I . The only difference is that it does not partition the action space and therefore the number of neurons in its output layer is 56. Hyper-parameters remain consistent across the three models (DQN, DDQN and MAN): the discount is 0.99; the greedy-exploration ϵ linearly decreases from 1 to 0.1 in the first 10000 steps and keeps 0.1 afterwards; the batch size is 32; the soft-update index is 0.005; the learning rates are adjusted to the respective optimal values based on the results of several experiments. As for the reward function, we refer to the paper by Junhao Zhang *et al.* [30]. The whole process is trained in the Pybullet simulator [31].

The results are shown in the Figure 3. The bumpiness is an indicator calculated by the variance of the outline (marked with blue line in the Figure 3), the smaller the number, the flatter the top layer of the pile. Within the same training episodes, DQN learned almost no reasonable policy; DDQN learned a good but still imperfect policy; and MAN learned an optimal policy, which outputs the lowest height and bumpiness.

B. General Atari Game-Playing

We further evaluated our proposed method on the Arcade Learning Environment (ALE) [32], to confirm MAN's capacity to tackle more complicated problems. The goal is to use a single algorithm and architecture with a defined set of hyper-parameters to learn to play all of the games using only raw pixel observations and game rewards. This environment is widely used as a benchmark in RL due to the high-dimensional observation and the enormous number of diverse games.

We chose 12 games that combine both button and joystick control, each with an action space of 18 dimensions. Both DQN and DDQN had difficulty mastering joystick and button control at the same time. However, with MAN, the agent first determines the direction of the joystick (9 actions in total), and then chooses to press or not press the button (2 actions in total). Thus, we reduce 18 actions to 11 (9+2) actions which reduces the exploration need.

In MAN learning, we use two networks, which are identical except the output layer, to estimate the value of joystick actions and button actions respectively. The network architecture has the same low-level convolutional structure of DQN (Mnih *et al.*, 2015; van Hasselt *et al.*, 2015). The input to the neural network is an $84 \times 84 \times 4$ image produced by the pre-process function. The first layer has 32 8×8 filters with stride 4, the second layer has 64 4×4 filters with stride 2, the third layer has 64 3×3 filters with stride 1, and the final layer is a fully-connected layer with 512 units. The output layer is a fully-connected linear layer with the size being the number of valid actions, which is 9 and 2 respectively. We adopt the hyper-parameters of van Hasselt *et al.* (2015), with the exception of the learning rate which we chose to be slightly higher. Additionally, we chose to use the Adam

optimizer [33] to optimize the networks rather than RMSprop [34], because it is more empirically stable.

In practice, we closely follow the setup of van Hasselt *et al.* [11], including frame-skipping technique and clipped reward, compare to their results using DQN and DDQN. Additionally, as in [11], we begin the game with up to 30 no-op actions to provide the agent with a random starting position. It is important to note that due to the limitation of computation resources, we only train MAN with 100M steps for each game, which is one-fifth of the original steps in the work of Hasselt *et al.*. The results shown of human performance as well as DQN and DDQN come directly from the work of [6].

In order to obtain a uniform standard to assess our method, we calculate the percentage (positive or negative) improvement in score over the best human agent scores using the following equation.

$$\frac{\text{Score}_{\text{Agent}} - \text{Score}_{\text{Random}}}{\text{Score}_{\text{Human}} - \text{Score}_{\text{Random}}}$$

Table I summarizes the outcomes for each game. Table II lists the normalized scores for each of the 12 games.

TABLE I

MEAN AND MEDIAN SCORES ACROSS ALL 12 ATARI GAMES, MEASURED IN PERCENTAGES OF HUMAN PERFORMANCE.

	Mean	Median
DQN	261.0%	87.3%
DDQN	282.0%	93.2%
MAN(ours)	397.7%	128.5%

TABLE II

NORMALIZED RESULTS FOR THE NO-OP EVALUATION CONDITION

Game	DQN	DDQN	MAN
Boxing	1707.86%	1942.86%	2239.29 %
Chopper Command	64.78%	42.36%	72.88%
Fishing Derby	95.16%	115.23%	111.11%
Frostbite	6.16%	4.13%	179.67%
H.E.R.O	76.5%	78.15%	79.6%
Ice Hockey	79.34%	72.73%	54.55%
James Bond	145.00%	108.29%	145.88%
Krull	277.01%	350.08 %	989.58%
Private Eye	2.53%	0.93%	0.11%
Robotank	508.97%	458.76%	581.96%
Seaquest	25.94%	39.41%	55.59%
Tennis	143.15%	171.14%	265.77%

Note: In above two tables, DQN and DDQN as given by Hasselt *et al.* (2016). The MAN only trained 10 million steps, instead DQN and DDQN trained 50 million steps.

Using this performance measure, it is clear that the MAN learning performs significantly better than both DQN and DDQN. Noteworthy examples include Frostbite (from 6.16%/4.13% to 179.67%), Krull (from 277.01%/350.08% to 989.58%), Seaquest (from 25.94%/39.41% to 55.59%), and Tennis (from 143.15%/171.14% to 265.77%). Figure 4 visualizes the improvement of the MAN over the baseline

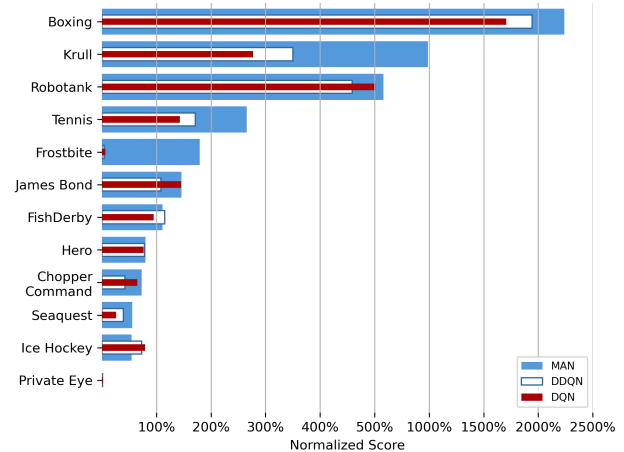


Fig. 4. Scores on 12 Atari games were normalized and tested for 20 episodes per game with human starts. The results of DQN and DDQN come from Hasselt *et al.* (2016).

DQN and DDQN. Once again, it needs to be reiterated that this was not a fair game: we only trained for one-fifth of the time compared to the baselines. However, even with this hindrance, we still notice that MAN outperformed the baselines on the vast majority of games. In fact, MAN outperforms DQN in 83.3 percent of games (10 out of 12). It also outperforms the DDQN in 75 percent (9 out of 12) of the games. On 6 of 12 games, our system achieves human-level performance. On most games the improvements from DQN/DDQN to MAN are striking, in many cases bringing scores much closer to human, or even surpassing these. Thus, we assume that if we had been able to train MAN for the same number of timesteps, our results would be even better.

VI. CONCLUSION

We introduced MAN, a novel neural network architecture build off of deep Q-networks that splits the original action into two sub-actions, while sharing a common feature learning module. This method, in combination with some algorithmic improvements, leads to dramatic improvements over existing approaches for DRL in the challenging domain of large action spaces. This improvement is due to two main aspects of our approach. Firstly, MAN decreases the action space, which in turn simplifies exploration. Secondly, within every update in MAN, we update the Q values twice within two smaller action spaces. Therefore, not only does our approach have more frequent updates, it also has the advantage of being easier to explore. This phenomenon is reflected in the experiments, where the advantage of the MAN over single-stream Q networks is tremendous.

We anticipate the greatest potential of this method lies in the domain of image-based action spaces, since we can very easily reduce the action space of an image of length M and width N from $M \times N$ to $M + N$. In the future, we plan to expand the usability of our algorithm to more complicated settings, such as image-based pick and place problems. We also aim to investigate how we can make use of the proposed method for controlling real-world systems.

REFERENCES

[1] V. Mnih, K. Kavukcuoglu, D. Silver, A. Graves, I. Antonoglou, D. Wierstra, and M. Riedmiller, “Playing atari with deep reinforcement learning,” *arXiv preprint arXiv:1312.5602*, 2013.

[2] V. Mnih, K. Kavukcuoglu, D. Silver, A. A. Rusu, J. Veness, M. G. Bellemare, A. Graves, M. Riedmiller, A. K. Fidjeland, G. Ostrovski *et al.*, “Human-level control through deep reinforcement learning,” *nature*, vol. 518, no. 7540, pp. 529–533, 2015.

[3] G. Dulac-Arnold, R. Evans, H. van Hasselt, P. Sunehag, T. Lillicrap, J. Hunt, T. Mann, T. Weber, T. Degrif, and B. Coppin, “Deep reinforcement learning in large discrete action spaces,” *arXiv preprint arXiv:1512.07679*, 2015.

[4] R. S. Sutton, D. McAllester, S. Singh, and Y. Mansour, “Policy gradient methods for reinforcement learning with function approximation,” *Advances in neural information processing systems*, vol. 12, 1999.

[5] R. S. Sutton, “Learning to predict by the methods of temporal differences,” *Machine learning*, vol. 3, no. 1, pp. 9–44, 1988.

[6] H. Van Hasselt, A. Guez, and D. Silver, “Deep reinforcement learning with double q-learning,” in *Proceedings of the AAAI conference on artificial intelligence*, vol. 30, no. 1, 2016.

[7] G. Tesauro *et al.*, “Temporal difference learning and td-gammon,” *Communications of the ACM*, vol. 38, no. 3, pp. 58–68, 1995.

[8] C. J. C. H. Watkins and P. Dayan, “Technical note: q -learning,” *Mach. Learn.*, vol. 8, no. 3–4, p. 279–292, may 1992. [Online]. Available: <https://doi.org/10.1007/BF00992698>

[9] C. J. Watkins and P. Dayan, “Q-learning,” *Machine learning*, vol. 8, no. 3, pp. 279–292, 1992.

[10] Z. Wang, T. Schaul, M. Hessel, H. Hasselt, M. Lanctot, and N. Freitas, “Dueling network architectures for deep reinforcement learning,” in *International conference on machine learning*. PMLR, 2016, pp. 1995–2003.

[11] M. Hessel, J. Modayil, H. Van Hasselt, T. Schaul, G. Ostrovski, W. Dabney, D. Horgan, B. Piot, M. Azar, and D. Silver, “Rainbow: Combining improvements in deep reinforcement learning,” in *Thirty-second AAAI conference on artificial intelligence*, 2018.

[12] F. S. He, Y. Liu, A. G. Schwing, and J. Peng, “Learning to play in a day: Faster deep reinforcement learning by optimality tightening,” *arXiv preprint arXiv:1611.01606*, 2016.

[13] M. Hausknecht and P. Stone, “Deep recurrent q-learning for partially observable mdps,” in *2015 aaai fall symposium series*, 2015.

[14] O. Anschel, N. Baram, and N. Shimkin, “Averaged-dqn: Variance reduction and stabilization for deep reinforcement learning,” in *International conference on machine learning*. PMLR, 2017, pp. 176–185.

[15] M. Sabatelli, G. Louppe, P. Geurts, and M. A. Wiering, “Deep quality-value (dqv) learning,” *arXiv preprint arXiv:1810.00368*, 2018.

[16] J. Schulman, X. Chen, and P. Abbeel, “Equivalence between policy gradients and soft q-learning,” *arXiv preprint arXiv:1704.06440*, 2017.

[17] H. P. van Hasselt, A. Guez, M. Hessel, V. Mnih, and D. Silver, “Learning values across many orders of magnitude,” *Advances in neural information processing systems*, vol. 29, 2016.

[18] M. G. Bellemare, W. Dabney, and R. Munos, “A distributional perspective on reinforcement learning,” in *International Conference on Machine Learning*. PMLR, 2017, pp. 449–458.

[19] I. Osband, C. Blundell, A. Pritzel, and B. Van Roy, “Deep exploration via bootstrapped dqn,” *Advances in neural information processing systems*, vol. 29, 2016.

[20] W. Dabney, G. Ostrovski, D. Silver, and R. Munos, “Implicit quantile networks for distributional reinforcement learning,” in *International conference on machine learning*. PMLR, 2018, pp. 1096–1105.

[21] W. Dabney, M. Rowland, M. Bellemare, and R. Munos, “Distributional reinforcement learning with quantile regression,” in *Proceedings of the AAAI Conference on Artificial Intelligence*, vol. 32, no. 1, 2018.

[22] D. Horgan, J. Quan, D. Budden, G. Barth-Maron, M. Hessel, H. Van Hasselt, and D. Silver, “Distributed prioritized experience replay,” *arXiv preprint arXiv:1803.00933*, 2018.

[23] T. Pohlen, B. Piot, T. Hester, M. G. Azar, D. Horgan, D. Budden, G. Barth-Maron, H. Van Hasselt, J. Quan, M. Večerík *et al.*, “Observe and look further: Achieving consistent performance on atari,” *arXiv preprint arXiv:1805.11593*, 2018.

[24] T. Hester, M. Večerík, O. Pietquin, M. Lanctot, T. Schaul, B. Piot, D. Horgan, J. Quan, A. Sendonaris, I. Osband *et al.*, “Deep q-learning from demonstrations,” in *Proceedings of the AAAI Conference on Artificial Intelligence*, vol. 32, no. 1, 2018.

[25] A. Nair, P. Srinivasan, S. Blackwell, C. Alcicek, R. Fearon, A. De Maria, V. Panneershelvam, M. Suleyman, C. Beattie, S. Petersen *et al.*, “Massively parallel methods for deep reinforcement learning,” *arXiv preprint arXiv:1507.04296*, 2015.

[26] A. V. Clemente, H. N. Castejón, and A. Chandra, “Efficient parallel methods for deep reinforcement learning,” *arXiv preprint arXiv:1705.04862*, 2017.

[27] A. Stooke and P. Abbeel, “Accelerated methods for deep reinforcement learning,” *arXiv preprint arXiv:1803.02811*, 2018.

[28] L.-J. Lin, “Self-improving reactive agents based on reinforcement learning, planning and teaching,” *Machine learning*, vol. 8, no. 3, pp. 293–321, 1992.

[29] H. Hasselt, “Double q-learning,” *Advances in neural information processing systems*, vol. 23, 2010.

[30] J. Zhang, W. Zhang, R. Song, L. Ma, and Y. Li, “Grasp for stacking via deep reinforcement learning,” in *2020 IEEE International Conference on Robotics and Automation (ICRA)*. IEEE, 2020, pp. 2543–2549.

[31] E. Coumans and Y. Bai, “Pybullet, a python module for physics simulation for games, robotics and machine learning,” <http://pybullet.org>, 2016–2021.

[32] M. G. Bellemare, Y. Naddaf, J. Veness, and M. Bowling, “The arcade learning environment: An evaluation platform for general agents,” *Journal of Artificial Intelligence Research*, vol. 47, pp. 253–279, 2013.

[33] D. P. Kingma and J. Ba, “Adam: A method for stochastic optimization,” *arXiv preprint arXiv:1412.6980*, 2014.

[34] T. Tieleman and G. Hinton, “Lecture 6.5-rmsprop: Divide the gradient by a running average of its recent magnitude.” *COURSERA: Neural Networks for Machine Learning*, 4, 26–31, 2012.